Supramolecular Chemistry
Publication details, including instructions for authors and subscription information:
http://www.informaworld.com/smpp/title~content=t713649759

Polymerisation of an Anionic Monomer in a Self-Assembled $M_{12}L_{24}$ Coordination Sphere with Cationic Interior

Takashi Kikuchi[a]; Takashi Murase[a]; Sota Sato[a]; Makoto Fujita[a]
[a] Department of Applied Chemistry, School of Engineering, The University of Tokyo, Tokyo, Japan

To cite this Article Kikuchi, Takashi , Murase, Takashi , Sato, Sota and Fujita, Makoto(2008) 'Polymerisation of an Anionic Monomer in a Self-Assembled $M_{12}L_{24}$ Coordination Sphere with Cationic Interior', Supramolecular Chemistry, 20: 1, 81 — 94
To link to this Article: DOI: 10.1080/10610270701742579
URL: http://dx.doi.org/10.1080/10610270701742579

Supramolecular Chemistry, January–March 2008 Vol. 20 (1–2), pp. 81–94

Taylor & Francis
Taylor & Francis Group

Polymerisation of an Anionic Monomer in a Self-Assembled $M_{12}L_{24}$ Coordination Sphere with Cationic Interior

TAKASHI KIKUCHI, TAKASHI MURASE, SOTA SATO and MAKOTO FUJITA*

Department of Applied Chemistry, School of Engineering, The University of Tokyo, 7-3-1 Hongo, Bunkyo-ku, Tokyo, Japan

(Received 2 August 2007; Accepted 11 October 2007)

Polymerisation within a well-defined nanocavity leads to the precise control of the rate of polymerisation and the molecular weight of the resultant polymer. We prepared a highly cationic spherical complex that was self-assembled from 12 palladium(II) ions and 24 quaternary ammonium-attached bidentate ligands. NMR experiments confirmed that this spherical complex encapsulates multivalent anions within the cavity. When the free radical polymerisation of an anionic monomer, sodium *p*-styrenesulphonate, was carried out in the presence of the cationic sphere as a template, acceleration of the polymerisation and control of the molecular weight of the resultant polymer were observed. The molecular weight of the polymer depends on the number of the positive charges on the template.

Keywords: Self-assembly; Cage compounds; Cationic hosts; Electrostatic interaction; Template polymerisation

INTRODUCTION

Electrostatic interaction between cations and anions is one of the fundamental interactions and can exert its strong power, depending on the surrounding dielectric constant, not only in organic solvents but also in water. In nature, electrostatic interaction plays an important role in the recognition and interaction of bioorganic polymers and aggregates, such as DNA and lipid bilayers. For example, virus protein cages, capsids, have highly positively charged interior surfaces [1, 2]. They are composed of cationic amino residues that project into the interior and serve to store and transport organic polymers of nucleic acids. The tightly packed cationic residues encapsulate the nucleic acids via cooperative electrostatic interaction with the anionic phosphate backbones of the nucleic acids and stabilise the whole structure.

Cationic micelles are another molecular assembly. They are composed of numerous cationic surfactants typically having a long alkyl chain tail and a quaternary ammonium cation head [3]. The cationic polar heads in micelles face outwards in water and hydrophobic molecules can be incorporated into the interior hydrophobic environment. The application of cationic micellar aggregates goes beyond the usage as mere hosts. By using cationic micellar rod arrays as removable templates, mesoporous silica with hexagonally packed cylindrical shapes can be obtained [4, 5]. The cationic organic templates align the anionic inorganic monomers, orthosilicates, on the surfaces and allow the condensation reaction to give polymeric silicates [6]. In this way, fascinating (poly)cationic materials have received much attention, as a consequence of their potential to gather anionic monomers and regulate the resulting anionic polymer [6–14].

Matrix (template) polymerisation of *p*-styrenesulphonic acid anions on polycationic backbones is another practical example of effective electrostatic interactions [15–18]. In the preparation of poly(styrenesulphonic acid) counterions, a strong rate-enhancing effect is produced by the polycationic templates. It was shown that the polymerising monomeric counterions are not rigidly attached to the charged sites on the cationic matrix but have substantial motional freedom along the templates. The drastic increase in the polymerisation rate was ascribed to the phenomenon of 'counterion condensation' on the templates. However, the existing artificial polycationic templates do not have well-defined chemical structures and cannot offer spatially restricted regions like virus capsids.

*Corresponding author. E-mail: mfujita@appchem.t.u-tokyo.ac.jp

ISSN 1061-0278 print/ISSN 1029-0478 online © 2008 Taylor & Francis
DOI: 10.1080/10610270701742579

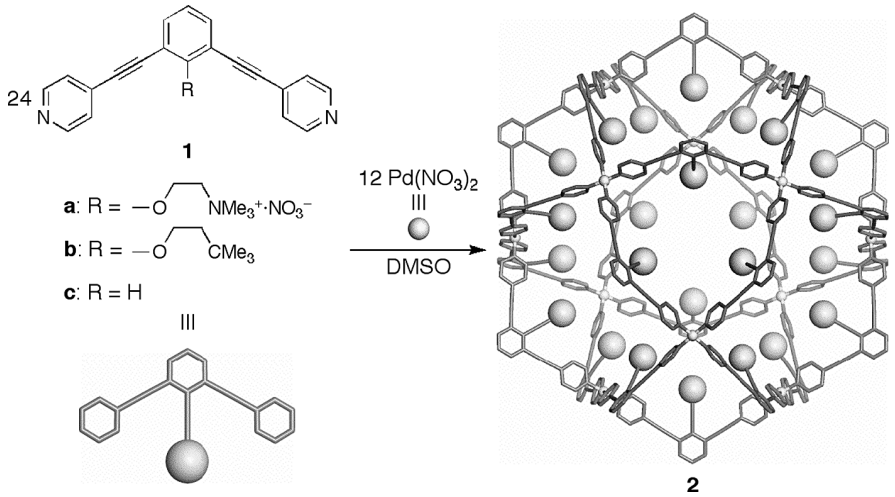

SCHEME 1 Self-assembly of $M_{12}L_{24}$ spherical complexes **2** with 24 ammonium cations internally (**2a**) and without cationic moieties (**2b**, **2c**).

These self-assembled biomacromolecular architectures can serve as not only nanoreactors or nanotemplates for crystallisations and other reactions [19–25], but also nanoscaffolds for the attachment of new chemical functionalities [25–31].

We have demonstrated that capsid-like hollow cages, $M_{12}L_{24}$ spheres, can be prepared in quantitative yield from 36 components, i.e. 12 metal ions (M) and 24 bridging ligands (L) [32–37]. The internal environment of these compounds can be finely tuned by attaching a functional group to the ligands before the self-assemble process [33–35, 37]. We report herein the construction of a highly cationic nanoenvironment, where 24 ammonium cations coat the interior surfaces of spherical cages (Scheme 1). We demonstrate that (poly)anionic guest molecules are encapsulated and show spatially controlled radical polymerisation of anionic sodium *p*-styrenesulphonates within the sphere.

RESULTS AND DISCUSSION

Synthesis and Characterisation of Spherical Complexes 2

Quaternary ammonium cation-attached ligand **1a** was synthesised as follows (Scheme 2). 2,6-Dibromophenol was heated with 2-(dimethylamino)ethyl chloride hydrochloride and K_2CO_3 in DMF to

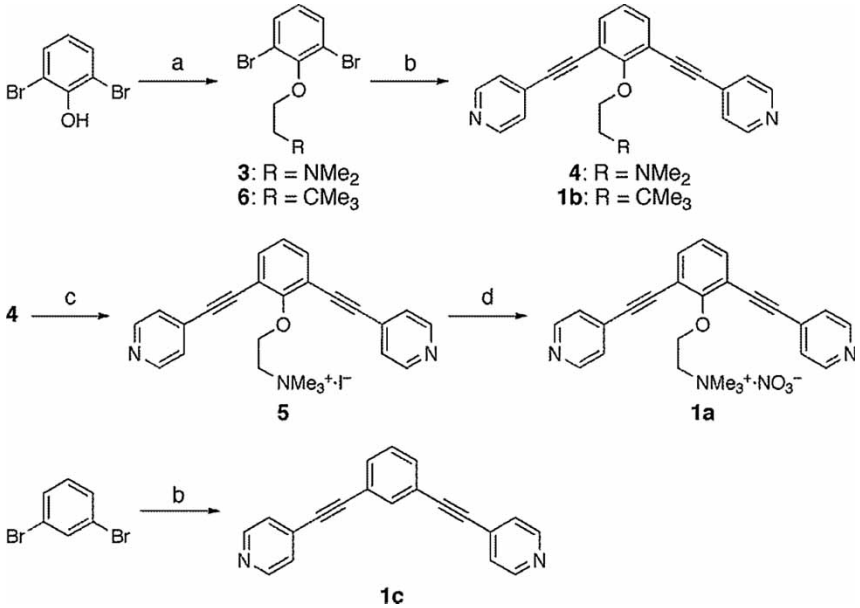

SCHEME 2 Synthesis of ligands **1a**–**c**. *Reagents and conditions:* (a) $ClCH_2CH_2NMe_2$ HCl (for **3**), $TsOCH_2CH_2CMe_3$ (for **6**), K_2CO_3, DMF, 90°C, 82% (for **3**), 95% (for **6**); (b) 4-ethynylpyridine hydrochloride, $PdCl_2(PhCN)_2$, P(*t*-Bu)$_3$, CuI, HN(*i*-Pr)$_2$, 45°C, 75% (for **4**), 79% (for **1b**), 81% (for **1c**); (c) MeI, CH_3CN, RT, 90%; (d) $AgNO_3$, H_2O, 90°C, 71%.

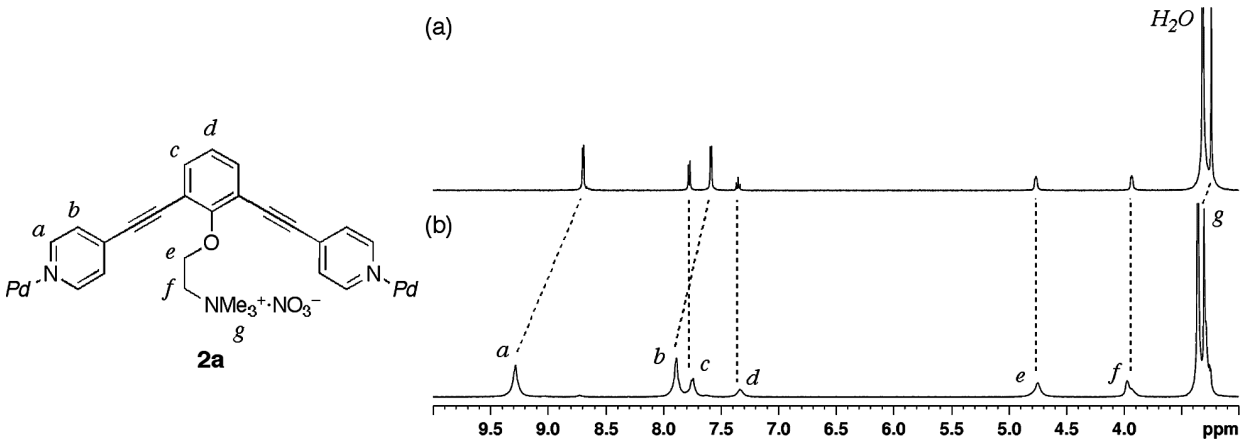

FIGURE 1 ^{1}H NMR spectra of (a) ligand **1a** and (b) complex **2a** (500 MHz, DMSO-d_6, 300 K, TMS).

give *N*,*N*-dimethylamino derivative (**3**) in 82% yield. Sonogashira cross-coupling of **3** with 4-ethynylpyridine in the presence of Pd(II) catalyst produced bis(pyridylethynyl)benzene (**4**) in 75% yield. The dimethylamino group of **4** was selectively methylated with methyl iodide (0.95 equiv.) in acetonitrile at room temperature [38] to give quaternary ammonium salt (**5**) in 90% yield. To depress the coordinating ability of the anion, the counteranion exchange with silver nitrate gave ligand **1a** in 71% yield.

Neutral ligands **1b** and **1c** were prepared in a similar way to ligand **1a**. A *tert*-butyl group is comparable in bulkiness to a trimethylamino group. Therefore, the spheres **2a** and **2b** should have the same size of the inner space.

When a mixture of ligand **1a** (7.0 μmol) and $Pd(NO_3)_2$ (3.5 μmol) in DMSO-d_6 (0.7 ml) was heated at 70°C for 2 h, the quantitative construction of sphere **2a** was confirmed by ^{1}H NMR spectroscopy (Fig. 1). The notable downfield shifts of the signals of the protons on the pyridine rings (e.g. $\Delta\delta_{Py\alpha} = 0.59$ ppm) result from the formation of coordination bonds between metals and ligands. The number of the signals that was not changed after complexation indicates a highly symmetrical structure.

Diffusion-ordered NMR spectroscopy (DOSY) is a powerful method to separate signals from complex mixtures according to the diffusion coefficient (*D*) values [39]. The DOSY spectrum of complex **2a** shows a single band at $4.7 \times 10^{-11}\,m^2\,s^{-1}$, which is smaller than that of the ligand **1a** ($2.0 \times 10^{-10}\,m^2\,s^{-1}$; Fig. 2). These spectra support the quantitative formation of complex **2a** and are in good agreement with those of the $M_{12}L_{24}$ spheres reported previously [32–37]; see supplementary materials, Figs. S1–4).

After anion exchange from NO_3^- to OTf^-, cold-spray ionisation mass spectrometry (CSI-MS) [40,41] for complex **2a** clearly indicated an $M_{12}L_{24}$ composition with the molecular weight of 17611 Da by a series of $[M - n(OTf^-)]^{n+}$ ($n = 7$–11) peaks (Fig. 3). The lack of fragmentation indicates the remarkable stability of the complex. Elemental analysis also supported the $M_{12}L_{24}$ composition. Complexes **2b** and **2c** display similar properties (see supplementary materials).

The above NMR and CSI-MS measurements strongly indicate the formation of the spherical

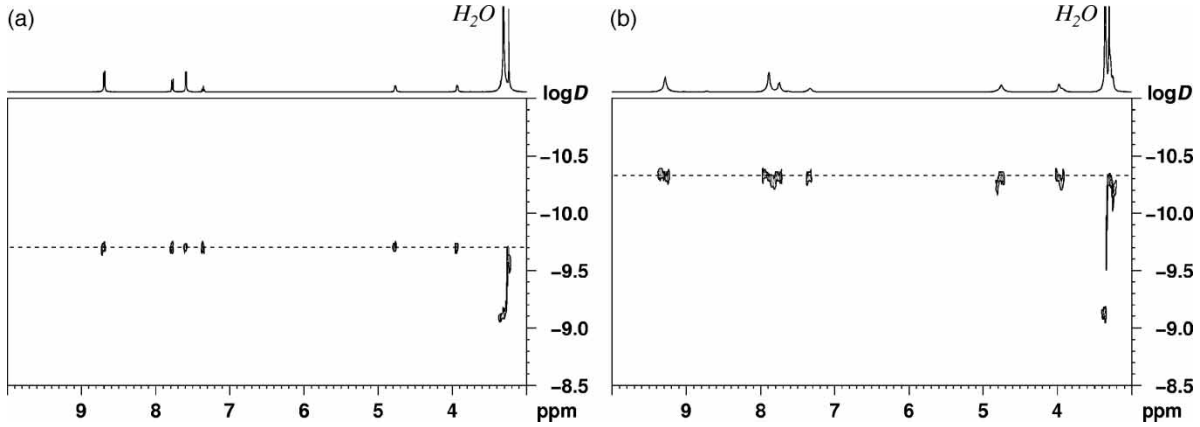

FIGURE 2 DOSY NMR spectra of (a) ligand **1a** and (b) complex **2a** (500 MHz, DMSO-d_6, 300 K, TMS).

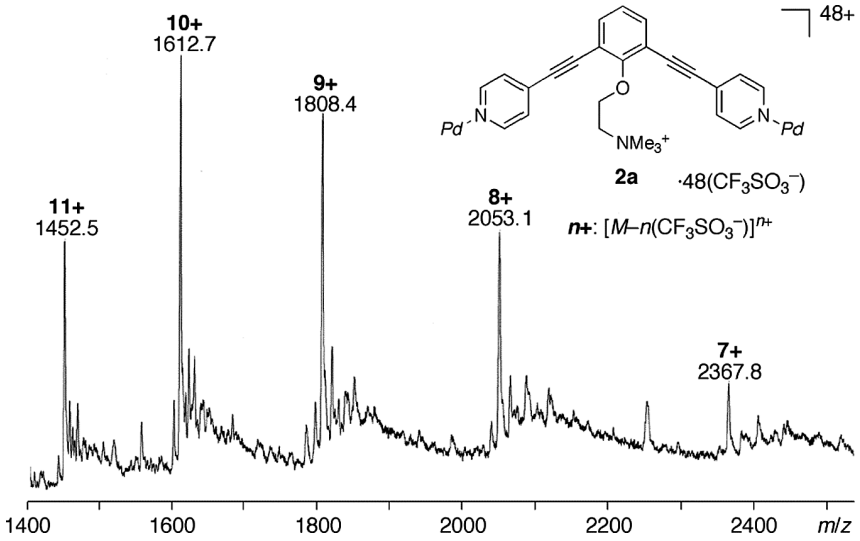

FIGURE 3 CSI-MS spectrum of complex **2a** ($CF_3SO_3^-$ salt, CH_3CN).

$M_{12}L_{24}$ complex **2a** (Fig. 4). The framework has cuboctahedron symmetry and a diameter of 4.6 nm. The cationic void has a diameter of approximately 2.3 nm and is accessible through the windows in the sphere framework. The void is coated with 24 cationic residues separated by approximately 0.6 nm, suggesting that multivalent interactions are possible within the cationic nanoenvironment.

Encapsulation of Anionic Guest Molecules into the Complex 2

We investigated the encapsulation of small anionic guest molecules within the cationic environment in the spherical complex **2a**. We found that carboxylate anions (e.g. sodium laurate, sodium terephthalate) and phosphate anions (e.g. sodium phenylphosphate, sodium thymidine-5′-phosphate) have destructive effects on the sphere because of their coordination on the Pd(II) ions. For this reason, sulphonate salts were chosen as anionic guests, because the coordination of sulphonate anions is negligible (Fig. 5).

We found that the cationic sphere **2a** strongly interacts with anionic guests **7a**–**c**, especially with multivalent anions, and incorporates them into the cationic interior in DMSO. When a DMSO solution of the sphere **2a** (0.208 mM) was treated with the dianionic guest disodium 2,7-naphthalenedisulphonate **7b** (8 equiv. for **2a**), the ^{1}H NMR spectrum showed downfield shifts for the anionic guest **7b** (e.g. $\Delta\delta^l_H = 0.17$ ppm), whereas the peaks of the sphere **2a**, especially the peak of the terminal N*Me*$_3$ proton, shifted upfield ($\Delta\delta_{NMe_3} = -0.07$ ppm; Fig. 6). In contrast, the addition of a monoanionic guest, sodium 2-naphthalenesulphonate **7a** (8 equiv. for **2a**) resulted in no detectable upfield shift of the peak of the N*Me*$_3$ proton. When only the ligand **1a** or $Pd(NO_3)_2$ was mixed with the dianionic guest **7b** in DMSO, no association was detectable by NMR. These results indicate that the incorporation of cationic residues within a hollow framework enables

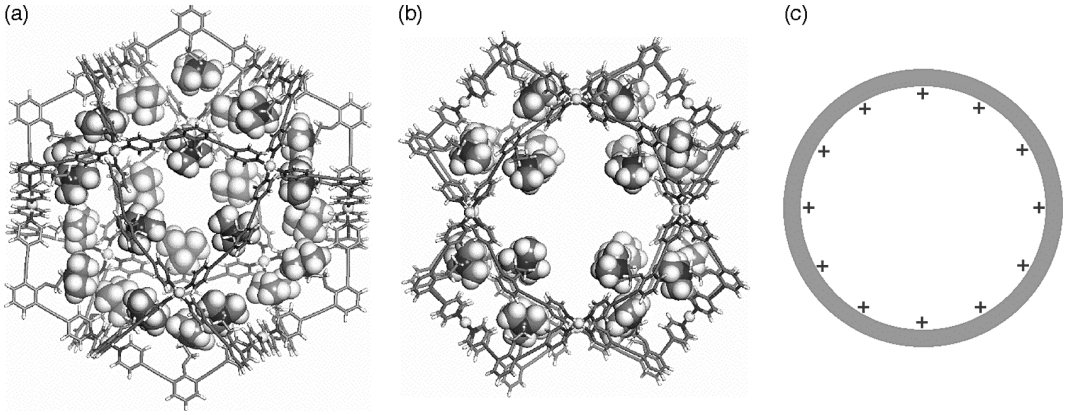

FIGURE 4 Molecular model of **2a** optimised by a force-field calculation of **2a** on MS Modelling 4.0 program. The representation viewed along a (a) three- and (b) fourfold axis. The terminal NMe_3 groups are shown in space-filling mode. (c) Schematic of **2a**.

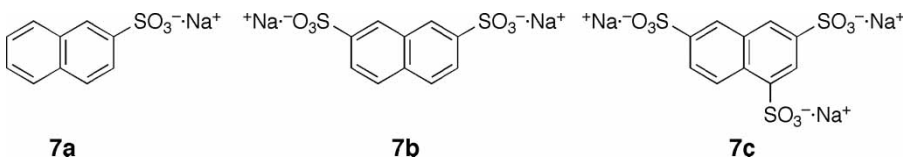

FIGURE 5 Sulphonate guest molecules having various numbers of negative charges.

electrostatic interactions with anionic guests in a multi-point fashion and that the strength of the cation–anion interaction strongly depends on the valence of anionic guests.

DOSY measurement was performed to evaluate the strength of the interaction between the cationic sphere **2a** and anionic guests. Fig. 7a shows that the D value of the free dianionic guest **7b** in DMSO ($D_{guest} = 2.2 \times 10^{-10}\,m^2\,s^{-1}$) is much larger than that of the spherical complex **2a** ($D_{complex} = 4.7 \times 10^{-11}\,m^2\,s^{-1}$). When the dianion **7b** (8 equiv. for **2a**) was added to the solution of the cationic sphere **2a** (0.208 mM), strong electrostatic interaction between the anionic guest and the cationic sphere restricted the motion of the guest, resulting in the dramatic decrease in D_{guest} and the similarity of D_{guest} to $D_{complex}$ (Fig. 7b). When trianionic **7c** was used as a guest, the electrostatic interactions were stronger and D_{guest} was equivalent to $D_{complex}$. This result implies tight encapsulation of the trianion **7c** within the cationic sphere **2a**. In contrast, monoanionic guest **7a** interacts weakly with the cationic sphere **2a**, which led to a large value of $D_{guest}/D_{complex}$. The $D_{guest}/D_{complex}$ values are summarised in Fig. 7c (see supplementary materials, Figs. S5–10). The above results clearly show that multivalent anions are more strongly bound by the cationic environment in the sphere **2a**.

Spherical cages **2b** and **2c** lack the pendant cationic residues but still possess 24 positive charges because 12 Pd(II) ions compose the cage framework. DOSY experiments revealed that there is an interaction between sphere **2c** and anionic guests. Comparison of the values of $D_{guest}/D_{complex}$ shows that the

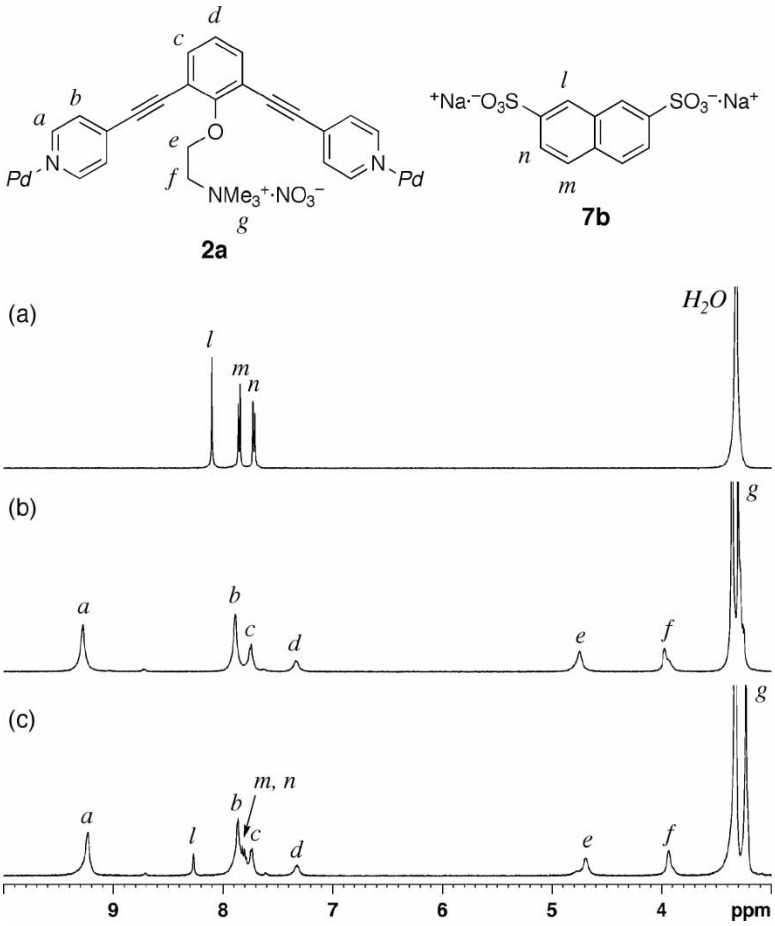

FIGURE 6 ^{1}H NMR spectra of (a) dianionic guest **7b**, (b) complex **2a** and (c) **2a** + **7b** (8 equiv.) (500 MHz, DMSO-d_6, 300 K, TMS).

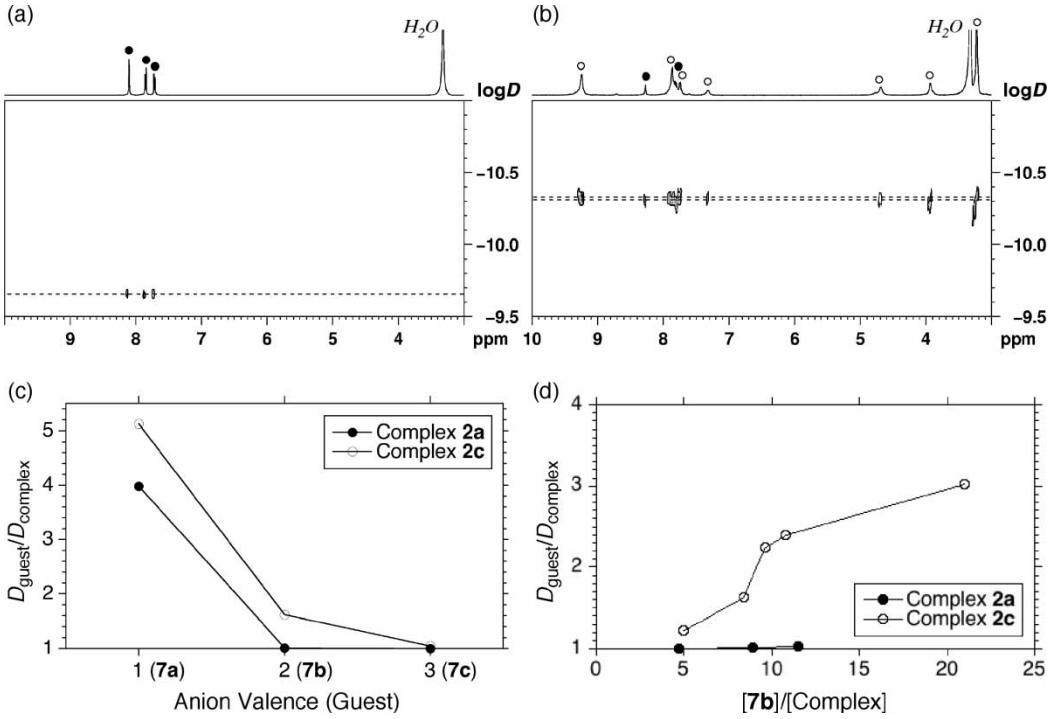

FIGURE 7 DOSY NMR spectra of (a) dianionic guest **7b** and (b) complex **2a** + **7b** (8 equiv.) (500 MHz, DMSO-d_6, 300 K, TMS; black circle, **7b**; white circle, **2a**). (c) Ratio of diffusion coefficients ($D_{guest}/D_{complex}$) for anionic guests **7a**–**c** in the presence of spherical complex **2a** or **2c** (8 equiv. guests for complex). (d) $D_{guest}/D_{complex}$ for the ratio of the concentration of guest **7b** to **2a** or **2c**.

interaction is weaker than the case of **2a** (Fig. 7c). The quaternary ammonium residues of **2a** play a significant role in the electrostatic interactions.

The amount of guests for spheres also affected the strength of the encapsulation. As the amount of the dianionic guest **7b** for sphere **2c** increased, the value of $D_{guest}/D_{complex}$ increased. On the other hand, the amount of **7b** for **2a** hardly affected the value of $D_{guest}/D_{complex}$, which was almost constant and close to 1 (Fig. 7d). When more than 15 equiv. of **7b** was added to **2a**, a precipitate was formed. The signals derived from sphere **2a** disappeared in the ^{1}H NMR spectrum. These results indicate the formation of a polycation/polyanion complex and support the reinforcement of the encapsulation by the internal cationic surface.

Polymerisation of an Anionic Monomer within the Complex 2

Given that the cationic sphere **2a** interacts strongly with polyanionic guests, it is expected that the polymerisation of an anionic monomer guest should occur within the sphere. Polymerisation within a well-defined isolated cavity can lead to a precise control of polymerisation, such as the molecular weight of the obtained polymer and the rate of the polymerisation.

Free radical polymerisation of an anionic monomer, sodium *p*-styrenesulphonate **8** (100 mM) [42–48], was carried out in the presence of the cationic nanosphere **2a** (0.417 mM) in DMSO at 70°C for 2 h using a redox initiator system, $(NH_4)_2S_2O_8$ (1.0 mM)–$NaHSO_3$ (1.1 mM) [49].[1] When the monomer **8** was dissolved in the solution of complex **2a**, the peak assigned to the NMe_3 group of **2a** shifted upfield ($\Delta\delta_{NMe_3} = -0.08$ ppm). This observation indicates a certain electrostatic interaction between the cationic sphere and the monoanionic monomer before the polymerisation when the large excess monomer **8** (*ca.* 240 equiv.) was added.[2] As the polymerisation proceeded, the solution became turbid and finally an insoluble powder precipitated. ^{1}H NMR measurement showed the disappearance of the peaks derived from the complex **2a** after the polymerisation. Although, broad signals of protons on sp^3 carbon atoms of poly(*p*-styrenesulphonate) (PSS) appear around 1–2 ppm, no peaks were observed in this region after polymerisation, and only the peaks attributed to the unreacted monomer

[1] $(NH_4)_2S_2O_8$ is a dianionic initiator and strongly encapsulated in the complex before polymerisation. Therefore, a radical species should be generated in the complex.

[2] When the amount of the monomer **8** was decreased (24 equiv.), there were no detectable upfield shifts of the peaks of the polycationic cage in the ^{1}H NMR spectrum. Therefore, some of the large excess anionic monomers **8** can be concentrated or trapped around the cationic spherical scaffold even though the interaction is weak.

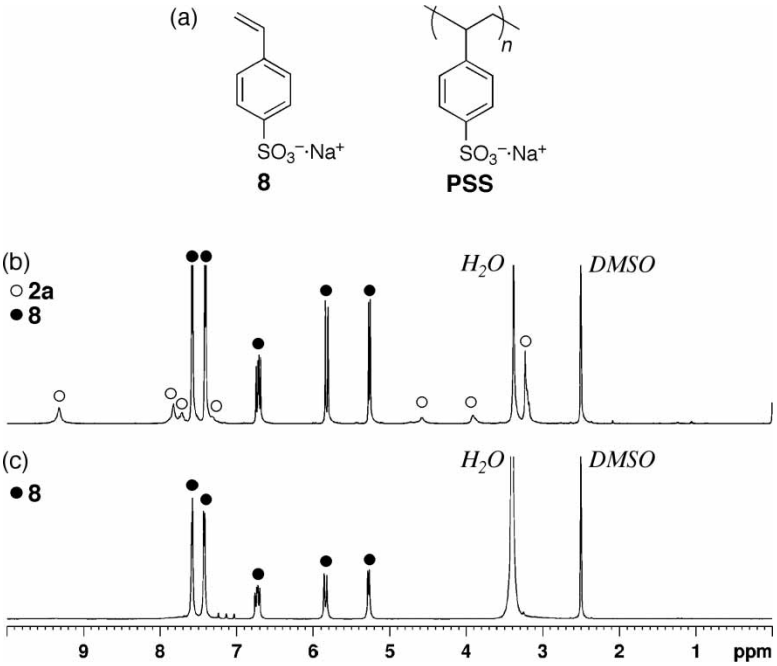

FIGURE 8 (a) Structures of anionic monomer **8** and PSS. ^{1}H NMR spectra (b) before and (c) after the polymerisation of **8** in the presence of complex **2a** at 70°C for 2 h (500 MHz, DMSO-d_6, 300 K, TMS).

8 were observed (Fig. 8). These results indicate that all of the produced PSS chains were incorporated into the sphere to form an insoluble polycation/polyanion complex and precipitated.

Monomer consumption ratio (conversion) of the polymerisation was monitored by ^{1}H NMR experiments. The conversion was calculated from the ratio of the integrated areas under the peaks corresponding to monomer **8** and those corresponding to residual DMSO as an internal standard, using the following equation:

$$\text{Conv.}[\%] = \left[1 - \frac{(A_{\text{monomer}}/A_{\text{DMSO}})_t}{(A_{\text{monomer}}/A_{\text{DMSO}})_0}\right] \times 100 \quad (1)$$

where $A_{\text{monomer},t}$ and $A_{\text{DMSO},t}$ denote the integrated areas of the peaks corresponding to monomer **8** (utilising the peak of the vinyl proton at 5.8 ppm) and residual DMSO at a given reaction time (t), respectively.

The cationic sphere **2a** accelerated the radical polymerisation at the initial stage but constrained the final conversion of the monomer, when compared with the polymerisation in the absence of the sphere **2a**. As shown in Fig. 9a, the initial rate in the presence of the sphere **2a** was over 6.0 mM min^{-1}, whereas in the absence of the sphere it was 1.5 mM min^{-1}. The sphere **2a** acted as a polycationic template and accelerated the polymerisation by over fourfold (the reaction in the presence of the sphere **2a** was so fast

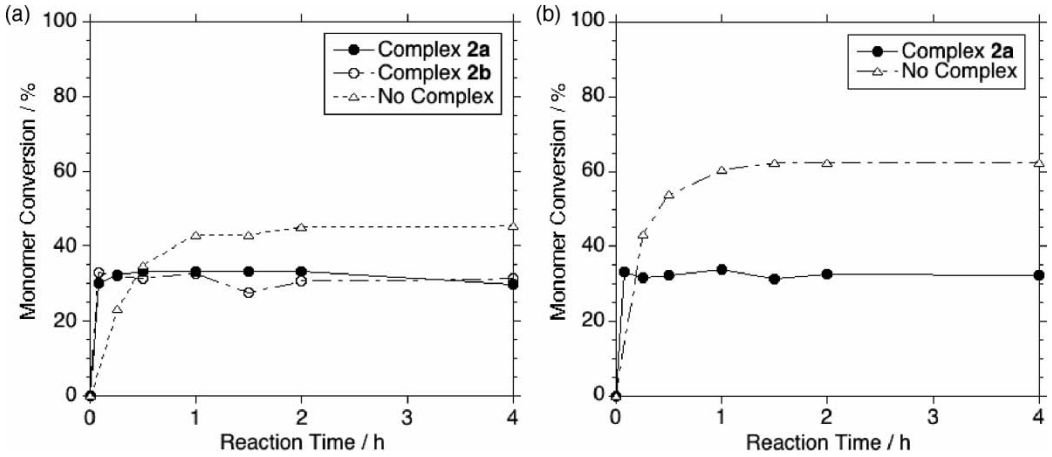

FIGURE 9 Changes of monomer conversion in the presence and absence of complex **2a** or **2b** as a function of time at 70°C. Redox initiator system, $(NH_4)_2S_2O_8$–$NaHSO_3$: (a) 1.0–1.1 mM; (b) 2.5–2.8 mM. See supplementary materials, Figures S11–15.

that the initial rate was underestimated). However, the final conversion of the monomer **8** was 30% in the presence of the complex **2a** but was 45% without the complex. This difference of the final conversions became more evident when the concentration of the redox initiator system, $(NH_4)_2S_2O_8$–$NaHSO_3$, was increased 2.5 times to be 2.5 mM–2.8 mM (Fig. 9b). In the absence of the complex **2a**, increasing the initiator system concentration increased the conversion to 62% but in the presence of the complex **2a**, the conversion remained constant. It is supposed that the growing polymer chain having multivalent negative charges is tightly incorporated within the sphere and hence that only the monomers **8** trapped in/around the cationic complex **2a** by electrostatic interaction polymerise rapidly. In addition, the precipitation of the polyelectrolyte complex including the growing polymer chain should prevent the frequent access of the monomer **8** to the radical centre of the polymer. As a result, the polymerisation rate of the anionic monomer **8** was accelerated but the conversion of the monomer was restricted by the cationic spherical complex **2a**.

The degree of polymerisation of the resultant anionic polymer (PSS) was examined by gel filtration chromatography (GFC) [45,46]. First, to isolate the resultant polymer, the precipitate was treated with an aqueous solution of excess ethylenediamine (en) to decompose the complex **2a**, leading to the removal of the Pd^{2+} ions as $[Pd(en)_2]^{2+}$ ions. Then, the insoluble mixture was filtered off and the filtrate, which contains the PSS, the ligand **1a** (cation) and the $[Pd(en)_2]^{2+}$, was chromatographed through a cation exchange resin (H-form) to remove cationic components. Finally, the acidic fraction was neutralised with aqueous NaOH and lyophilised to obtain a purified PSS as a pale brown solid.

The GFC analysis revealed that the PSS obtained from the reaction in the presence of complex **2a** (reaction condition: $(NH_4)_2S_2O_8$ (1.0 mM)–$NaHSO_3$ (1.1 mM), 70°C, 2 h; 30% conversion) had a number-average molecular weight (M_n) of 2860 relative to PSS standards and a polydispersity index (M_w/M_n; M_w denotes weight-average molecular weight) of 1.61 (Fig. 10b). In the absence of any template under the same reaction conditions, the values of M_n and M_w/M_n of the resultant polymer were 5800 and 3.53, respectively (Fig. 10a). The difference indicates that the well-defined cationic nanosphere **2a** controlled the number of the interacting anionic monomers **8** and that the polymerisation proceeded predominantly among the monomers trapped in/around the complex, resulting in the control of the molecular weight of the resultant polymer. The narrow distribution in the region of larger molecular weight in GFC profile verifies the restriction of the further reaction by the template. From the molecular weight of the monomer **8** (206.19) and a radical initiator species ($SO_4^{\cdot -}$; 96.06), the degrees of polymerisation of the obtained PSS were estimated to be 13.4 and 27.7 in the presence and absence of the sphere **2a**, respectively.

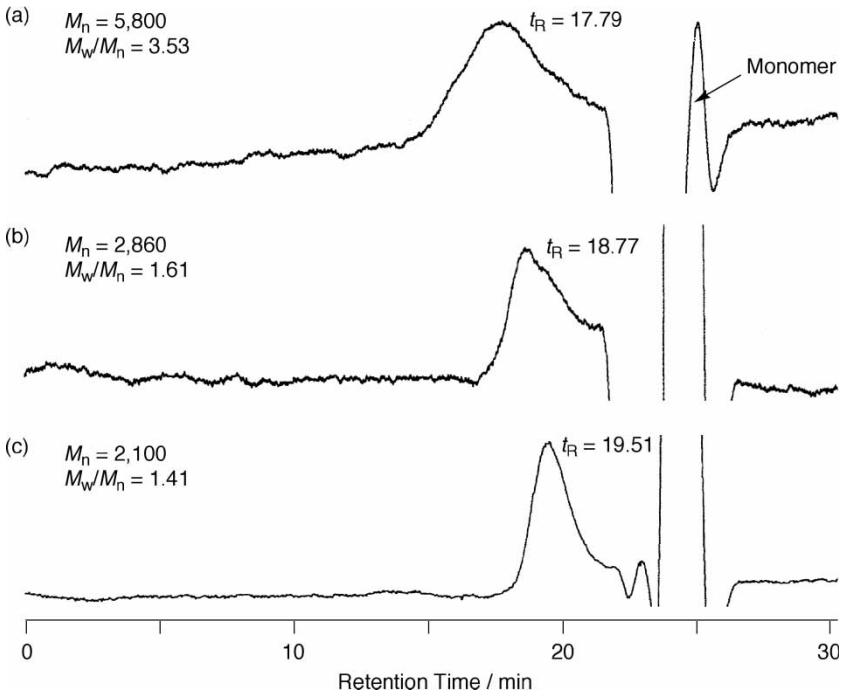

FIGURE 10 GFC profiles of PSS obtained in the presence of (a) no complex, (b) complex **2a** and (c) complex **2b**. For the detail of GFC conditions, see experimental section.

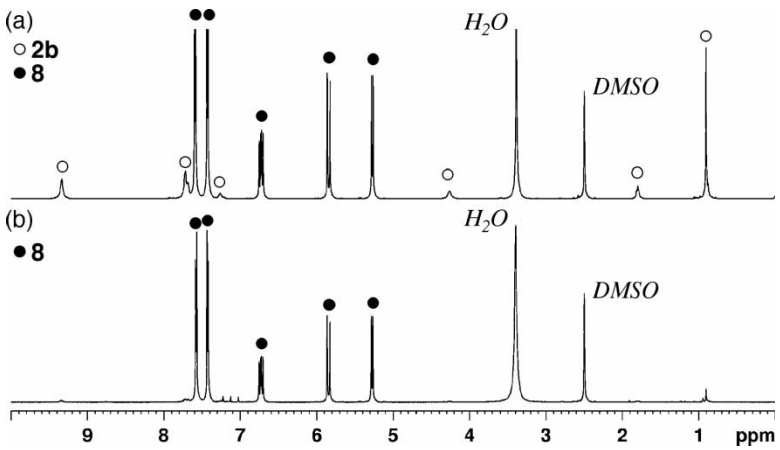

FIGURE 11 ^{1}H NMR spectra (a) before and (b) after the polymerisation of **8** in the presence of complex **2b** (500 MHz, DMSO-d_6, 300 K, TMS).

As a control experiment, the polymerisation of the monomer **8** was carried out in the presence of the spherical complex **2b** which does not have quaternary ammonium residues. NMR measurements revealed that the sphere **2b** also accelerated the polymerisation reaction and restricted the final conversion of the monomer **8**. NMR spectra before and after the polymerisation indicate that an insoluble polyelectrolyte complex between the resultant polymer and the sphere **2b** formed as the reaction proceeded (Fig. 11). The consumption of the monomer in the presence of the complex **2b** was faster than the case without the sphere, and the acceleration effect was comparable to that of the complex **2a** (Fig. 9a). Moreover, the final conversion of the monomer **8** was restricted to 30% and similar to the case of the cationic complex **2a**. Although, the sphere **2b** does not have any cationic residues, the framework of the sphere has 24 positive charges on the palladium coordination centres. It is concluded that this polycationic framework interacted with the growing polymer chain and the monomer **8**, resulting in the acceleration and the conversion control of the polymerisation.

GFC analysis revealed that the molecular weights of the resultant polymers largely depend on the number of the cations on the templates. For the PSS obtained from the polymerisation in the presence of the sphere **2b**, the values of M_n and M_w/M_n were 2100 (9.7 mer) and 1.41, respectively (Fig. 10c).

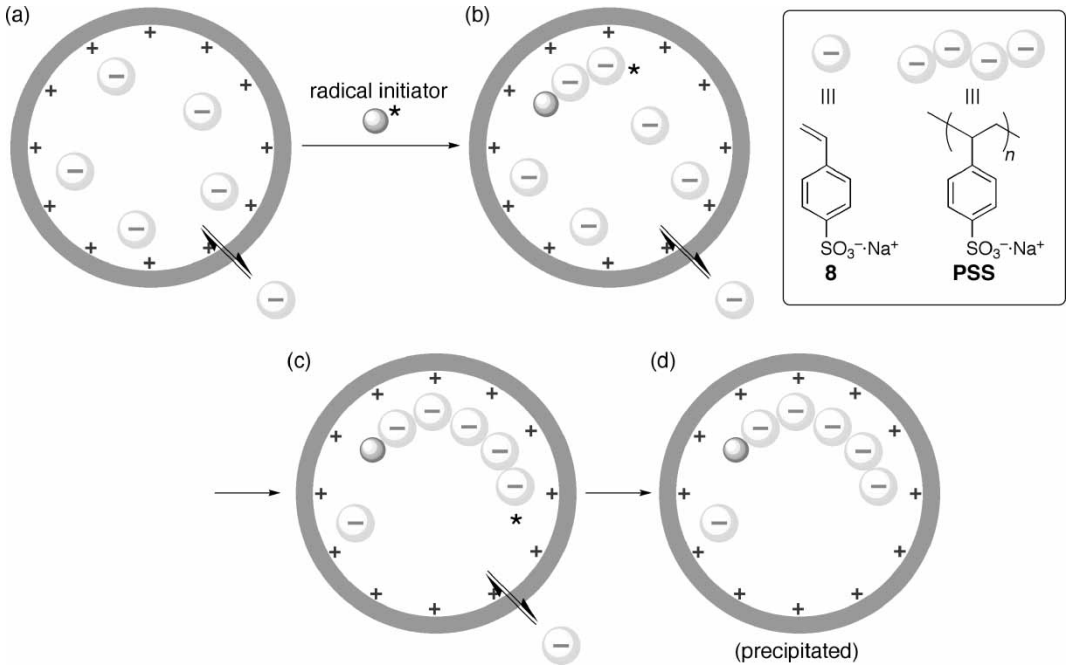

FIGURE 12 Schematic image of template radical polymerisation of anionic monomers **8** in a cationic nanosphere: (a) concentration of anionic monomers, (b) encapsulation of the growing polymer chain, (c) rapid polymerisation of the trapped monomers, (d) inhibition of further polymerisation of the polyelectrolyte complex. Asterisk (*) indicates a radical centre.

The molecular weight of the obtained PSS was restricted and the distribution was considerably narrowed, when compared with the case of no templates. Therefore, the complex **2b** also has the effect of controlling molecular weight on the polymerisation of the anionic monomer **8**. In addition, the degree of polymerisation of the polymer obtained in the presence of sphere **2b** was even smaller than that in the case of the cationic sphere **2a**. This result indicates that there is a strong correlation between the molecular weight of the resultant PSS and the number of the positive charges on the template; the number of the positive charges affects the number of the monomers trapped in/around the complex. Thus, we succeeded in controlling the molecular weight of the PSS by modifying the number of cations on the template.

Considering the above experiments, we propose that the polymerisation in the presence of the sphere proceeds in the following mechanism (Fig. 12). The anionic monomers **8** were concentrated on the cationic scaffold of the sphere via electrostatic interactions ('counterion condensation') (Fig. 12a). When the polymerisation was initiated, the growing polymer chain having multivalent negative charges was tightly incorporated into the polycationic nanocavity, where the monomers were concentrated (Fig. 12b). As a result, polymerisation proceeded rapidly among the trapped monomers (Fig. 12c) and the polymerisation reaction was accelerated. The formation of the insoluble polyelectrolyte complex prevented further reaction, resulting in the restriction of the monomer conversion (Fig. 12d). As a whole, polymerisation predominantly occurs among the trapped monomers and the degree of polymerisation of the resultant polymer can be controlled by the number of the trapped monomers, which is controlled by the number of positive charges on the template.

CONCLUSION

We succeeded in the preparation of the structurally well-defined cationic spherical complex **2a** bearing 24 cationic residues on its inner surface. The complexes have the ability to concentrate anionic guest molecules within the interior nanoenvironment. The strength of electrostatic interaction between the cationic nanocage and the anionic guests largely depends on their respective charges. We found that spheres **2a** and **2b** accelerated the radical polymerisation of an anionic monomer and controlled the molecular weight of the resultant polymer, depending on the number of positive charges on the template. Because the monomer units are concentrated *noncovalently*, it is possible to apply this polymerisation method to a wide range of anionic monomers without any modification of the template.

EXPERIMENTAL

General

NMR spectra were recorded on Bruker DRX-500 and AV-500 (500 MHz) spectrometers. All NMR spectral data were collected at 300 K and the chemical shift values reported here are with respect to an internal TMS standard for $CDCl_3$ and DMSO-d_6. GC–MS spectrum was measured on Agilent Technologies 5973N spectrometer. MALDI-TOF (LD +, dithranol) mass spectra were recorded on Applied Biosystems Voyager DE-STR. Cold-spray ionisation mass spectrometry (CSI-MS) spectra were measured on a four-sector (BE/BE) tandem mass spectrometer (JMS-700C, JEOL) equipped with a CSI source. IR measurements were carried out as KBr pellets using a Varian Scimitar FTS-2000 instrument. Cation exchange chromatography was conducted using Dowex MAC-3 resin. The number-average molecular weight (M_n) and polydispersity index (M_w/M_n) of the obtained and standard PSS were measured with gel filtration chromatography (GFC) (Japan Analytical Industry LC-918) with refractive index detection. The column was Shodex Asahipak GF-510HQ. The eluent, flow rate and temperature were 50 mM LiCl(aq.)/CH_3CN = 60:40, 0.5 ml/min and 30°C, respectively. Solvents and reagents were purchased from TCI CO., Ltd, WAKO Pure Chemical Industries Ltd and Sigma-Aldrich Co. Standard PSS oligomers (no. pss11114 ($M_p = 697$, $M_w/M_n < 1.20$); no. pss200504 ($M_p = 3420$, $M_w/M_n < 1.20$); no. pss8124 ($M_p = 6430$, $M_w/M_n < 1.20$); no. pss18061 ($M_p =$ 15,800, $M_w/M_n < 1.20$); no. pss16042 ($M_p = 33{,}500$, $M_w/M_n < 1.20$)) were purchased from Polymer Standards Service and a calibration curve was prepared using them. All the chemicals were of reagent grade and used without any further purification.

Synthesis of 1,3-dibromo-2-[2-(dimethylamino) ethoxy]benzene (3)

2,6-Dibromophenol (3.00 g, 11.9 mmol) was dissolved in DMF (100 ml). Potassium carbonate (8.30 g, 60.0 mmol) was added and the resulting mixture was stirred at 90°C. 2-(Dimethylamino)ethyl chloride hydrochloride (1.71 g, 11.9 mmol) was added in small portions for 1 h and the resulting mixture was stirred at 90°C for 19 h. The solvent was evaporated and the residue was dissolved in CH_2Cl_2. The CH_2Cl_2 suspension was washed with water and brine, dried over anhydrous Na_2SO_4, filtrated and concentrated *in vacuo*. The crude product was

purified by column chromatography on neutral silica gel ($CHCl_3$) to give **3** as a colourless oil (3.13 g, 9.72 mmol) in 82% yield: ^{1}H NMR (500 MHz, $CDCl_3$) δ: 7.50 (d, $J = 8.0$ Hz, 2H), 6.86 (t, $J = 8.1$ Hz, 1H), 4.11 (t, $J = 6.0$ Hz, 2H), 2.84 (t, $J = 6.0$ Hz, 2H), 2.39 (s, 6H). ^{13}C NMR (125 MHz, $CDCl_3$) δ: 153.4 (C), 132.7 (CH), 126.2 (CH), 118.5 (C), 70.8 (CH_2), 58.7 (CH_2), 45.8 (CH_3). IR (KBr, cm^{-1}): 2972, 2945, 2887, 2864, 2820, 2771, 1594, 1556, 1438, 1392, 1363, 1333, 1247, 1197, 1156, 1099, 1070, 1020, 997, 960, 903, 817, 768, 613, 525, 519, 414. GC–MS (EI) m/z: 323 $[M]^+$. Elemental anal. calcd for $C_{10}H_{13}Br_2NO$: C, 37.18; H, 4.06; N, 4.34. Found: C, 37.08; H, 4.06; N, 4.27.

Synthesis of 2-[2-(dimethylamino)ethoxy]-1,3-bis(4-pyridylethynyl)benzene (4)

Tri-*t*-butylphosphine (1.23 ml, 0.43 mmol; 10% solution in hexane) and diisopropylamine (2.50 ml, 17.6 mmol) were added to a mixture of compound **3** (1.11 g, 3.44 mmol), 4-ethynylpyridine hydrochloride (1.35 g, 9.64 mmol), $PdCl_2(PhCN)_2$ (80 mg, 0.21 mmol), copper(I) iodide (27 mg, 0.14 mmol) in degassed dioxane (10 ml). The reaction mixture was stirred at 45°C for 24 h under argon atmosphere. The mixture was diluted with ethyl acetate and filtrated. The ethyl acetate solution was washed with 10% ethylenediamine-containing water, water and brine, dried over anhydrous Na_2SO_4, filtrated and concentrated *in vacuo*. The crude product was purified by column chromatography on neutral silica gel (gradient elution from $CHCl_3$/MeOH = 100:0 to $CHCl_3$/MeOH = 96:4) to give **4** as a brown oil (944 mg, 2.57 mmol) in 75% yield: ^{1}H NMR (500 MHz, $CDCl_3$) δ: 8.63 (dd, $J = 4.5$, 1.6 Hz, 4H), 7.55 (d, $J = 7.8$ Hz, 2H), 7.41 (dd, $J = 4.4$, 1.6 Hz, 4H), 7.13 (t, $J = 7.8$ Hz, 1H), 4.40 (t, $J = 5.8$ Hz, 2H), 2.85 (t, $J = 5.8$ Hz, 2H), 2.36 (s, 6H). ^{13}C NMR (125 MHz, $CDCl_3$) δ: 161.7 (C), 149.9 (CH), 134.7 (CH), 131.2 (C), 125.5 (CH), 123.9 (CH), 117.0 (C), 91.3 (C), 89.7 (C), 72.6 (CH_2), 59.3 (CH_2), 45.9 (CH_3). IR (KBr, cm^{-1}): 2945, 2820, 2773, 2117, 1595, 1539, 1491, 1458, 1440, 1363, 1270, 1231, 1161, 1078, 1022, 990, 966, 906, 820, 790, 740, 548, 536, 505. MALDI-TOF MS m/z: 368 $[M + H]^+$. Elemental anal. calcd for $C_{24}H_{21}N_3O$ 0.2H_2O: C, 77.69; H, 5.81; N, 11.32. Found: C, 77.70; H, 6.03; N, 11.08.

Synthesis of Trimethyl[[2,6-bis(4-pyridylethynyl) phenoxy]ethyl]ammonium Iodide (5)

Methyl iodide (78.5 µl, 1.26 mmol) was added to a solution of compound **4** (489 mg, 1.33 mmol) in acetonitrile (20 ml). The reaction mixture was stirred at room temperature for 14 h under argon atmosphere. The solvent was evaporated and the residue was washed with ethyl acetate. The crude product was recrystallised from water to give **5** as a pale brown solid (577 mg, 1.13 mmol) in 90% yield: m.p. 205.5–206.2°C. ^{1}H NMR (500 MHz, DMSO-d_6) δ: 8.69 (d, $J = 5.6$ Hz, 4H), 7.78 (d, $J = 7.6$ Hz, 2H), 7.59 (d, $J = 5.8$ Hz, 4H), 7.35 (t, $J = 7.7$ Hz, 1H), 4.77 (t, $J = 4.4$ Hz, 2H), 3.93 (t, $J = 4.5$ Hz, 2H), 3.26 (s, 9H). ^{13}C NMR (125 MHz, DMSO-d_6) δ: 159.2 (C), 150.0 (CH), 135.4 (CH), 129.5 (C), 125.3 (CH), 125.1 (CH), 115.6 (C), 91.6 (C), 88.8 (C), 67.6 (CH_2), 64.7 (CH_2), 53.1 (CH_3). IR (KBr, cm^{-1}): 3040, 2981, 2212, 1652, 1599, 1541, 1491, 1476, 1443, 1407, 1385, 1374, 1339, 1227, 1207, 1089, 1053, 1001, 991, 954, 903, 877, 829, 794, 549, 536, 507, 472. MALDI-TOF MS m/z: 382 $[M - I]^+$. Elemental anal. calcd for $C_{25}H_{24}IN_3O$ 0.5AcOEt: C, 58.60; H, 5.10; N, 7.59. Found: C, 58.39; H, 5.11; N, 7.45.

Synthesis of Trimethyl[[2,6-bis(4-pyridylethynyl) phenoxy]ethyl]ammonium Nitrate (1a)

Compound **5** (200 mg, 0.392 mmol) and silver nitrate (66.7 mg, 0.393 mmol) were dissolved in water (30 ml). The reaction mixture was stirred in the dark at 90°C for 24 h. The solvent was evaporated and the residue was redissolved in $CHCl_3$. The precipitate was filtrated off and the filtrate was concentrated *in vacuo* to give **1a** as a brown powder (128 mg, 0.288 mmol) in 71% yield: m.p. 198.0–198.8°C. ^{1}H NMR (500 MHz, DMSO-d_6) δ: 8.69 (d, $J = 5.8$ Hz, 4H), 7.78 (d, $J = 7.6$ Hz, 2H), 7.59 (d, $J = 5.8$ Hz, 4H), 7.35 (t, $J = 7.6$ Hz, 1H), 4.77 (t, $J = 4.4$ Hz, 2H), 3.93 (t, $J = 4.5$ Hz, 2H), 3.26 (s, 9H). ^{13}C NMR (125 MHz, DMSO-d_6) δ: 159.2 (C), 150.0 (CH), 135.4 (CH), 129.5 (C), 125.2 (CH), 125.1 (CH), 115.6 (C), 91.6 (C), 88.8 (C), 67.6 (CH_2), 64.7 (CH_2), 53.1 (CH_3). IR (KBr, cm^{-1}): 3020, 2392, 2215, 1597, 1535, 1491, 1444, 1385, 1229, 1204, 1086, 1051, 997, 950, 905, 878, 826, 791, 537, 552. MALDI-TOF MS m/z: 382 $[M - NO_3]^+$. Elemental anal. calcd for $C_{25}H_{24}N_4O_4$: C, 67.55; H, 5.44; N, 12.60. Found: C, 67.29; H, 5.59; N, 12.32.

Synthesis of 3,3-dimethylbutyl *p*-toluenesulphonate

3,3-Dimethyl-1-butanol (5.00 ml, 41.3 mmol) and *p*-toluenesulphonyl chloride (15.7 g, 82.6 mmol) were dissolved in THF (180 ml). Triethylamine (34.4 ml, 248 mmol) was added slowly and the resulting mixture was stirred at 50°C for 12 h. The solvent was evaporated, the residue was dissolved in AcOEt and insoluble compounds were filtrated off. The filtrate was washed with water and brine, dried over anhydrous Na_2SO_4, filtrated and concentrated *in vacuo*. The crude product was purified by column chromatography on silica gel (gradient elution from hexane/AcOEt = 98:2 to hexane/AcOEt = 96:4) to give the title compound as a colourless oil (6.51 g, 25.4 mmol) in 61% yield: ^{1}H NMR (500 MHz, $CDCl_3$) δ: 7.79 (d, $J = 8.3$ Hz, 2H), 7.35 (d, $J = 8.0$ Hz, 2H),

4.09 (t, $J = 7.4$ Hz, 2H), 2.45 (s, 3H), 1.59 (t, $J = 7.4$ Hz, 2H), 0.88 (s, 9H). ^{13}C NMR (125 MHz, $CDCl_3$) δ: 144.8 (C), 133.4 (C), 129.9 (CH), 128.0 (CH), 68.5 (CH_2), 42.0 (CH_2), 29.8 (C), 29.6 (CH_3), 21.7 (CH_3). IR (KBr, cm^{-1}): 2958, 2871, 1599, 1476, 1363, 1307, 1248, 1186, 1176, 1098, 1032, 1020, 957, 892, 836, 816, 772, 744, 664. GC–MS (EI) m/z: 256 $[M]^+$. Elemental anal. calcd for $C_{13}H_{20}O_3S$: C, 59.75; H, 7.70. Found: C, 60.03; H, 7.67.

Synthesis of 1,3-dibromo-2-(3,3-dimethylbutoxy) benzene (6)

A similar procedure to that of **3** was employed to 3,3-dimethylbutyl *p*-toluenesulphonate (935 mg, 3.65 mmol) and 2,6-dibromophenol (1.01 g, 4.01 mmol) to give **6** as a colourless oil (1.17 g, 3.49 mmol) in 95% yield: ^{1}H NMR (500 MHz, $CDCl_3$) δ: 7.49 (d, $J = 8.0$ Hz, 2H), 6.84 (t, $J = 8.0$ Hz, 1H), 4.06 (t, $J = 7.6$ Hz, 2H), 1.87 (t, $J = 7.6$ Hz, 2H), 1.00 (s, 9H). ^{13}C NMR (125 MHz, $CDCl_3$) δ: 153.9 (C), 132.6 (CH), 126.0 (CH), 118.6 (C), 71.3 (CH_2), 43.1 (CH_2), 29.8 (C), 29.7 (CH_3). IR (KBr, cm^{-1}): 2956, 2868, 2366, 1555, 1477, 1441, 1384, 1366, 1242, 1200, 1177, 1070, 980, 937, 888, 836, 767, 723, 664. GC–MS (EI) m/z: 336 $[M]^+$. Elemental anal. calcd for $C_{12}H_{18}Br_2O$: C, 42.89; H, 4.80. Found: C, 42.92; H, 4.84.

Synthesis of 2-(3,3-dimethylbutoxy)-1,3-bis(4-pyridylethynyl)benzene (1b)

A similar procedure to that of **4** was employed to compound **6** (0.891 g, 2.65 mmol) and 4-ethynylpyridine hydrochloride (1.04 g, 7.43 mmol) to give **1b** as a pale yellow solid (798 mg, 2.10 mmol) in 79% yield: m.p. 78.0–78.9°C. ^{1}H NMR (500 MHz, DMSO-d_6) δ: 8.68 (d, $J = 5.2$ Hz, 4H), 7.70 (d, $J = 7.7$ Hz, 2H), 7.51 (d, $J = 5.7$ Hz, 4H), 7.27 (t, $J = 7.8$ Hz, 1H), 4.33 (t, $J = 7.2$ Hz, 2H), 1.82 (t, $J = 7.2$ Hz, 2H), 0.95 (s, 9H). ^{13}C NMR (125 MHz, DMSO-d_6) δ: 161.4 (C), 150.1 (CH), 135.0 (CH), 130.0 (C), 125.2 (CH), 124.4 (CH), 116.2 (C), 91.0 (C), 89.4 (C), 72.1 (CH_2), 43.0 (CH_2), 29.5 (CH_3), 29.5 (C). IR (KBr, cm^{-1}): 3042, 2953, 2868, 2216, 1593, 1539, 1489, 1442, 1405, 1382, 1235, 1208, 1083, 991, 972, 888, 821, 802, 737, 667. MALDI-TOF MS m/z: 381 $[M + H]^+$. Elemental anal. calcd for $C_{26}H_{24}N_2O$: C, 82.07; H, 6.36; N, 7.36. Found: C, 82.16; H, 6.55; N, 7.24.

Synthesis of 1,3-bis(4-pyridylethynyl)benzene (1c)

A similar procedure to that of **4** was employed to 1,3-dibromobenzene (0.645 g, 2.73 mmol) and 4-ethynylpyridine hydrochloride (1.07 g, 7.64 mmol) to give **1c** as a pale brown solid (0.620 g, 2.21 mmol) in 81% yield: m.p. 134.2–134.8°C. ^{1}H NMR (500 MHz, DMSO-d_6) δ: 8.84 (d, $J = 5.9$ Hz, 4H), 8.06 (s, 1H), 7.90 (d, $J = 9.3$ Hz, 2H), 7.75 (t, $J = 7.8$ Hz, 1H), 7.74 (d, $J = 5.9$ Hz, 4H). ^{13}C NMR (125 MHz, DMSO-d_6) δ: 150.9 (CH), 135.5 (CH), 133.5 (CH), 130.7 (C), 130.5 (CH), 126.3 (CH), 122.9 (C), 93.0 (C), 88.4 (C). IR (KBr, cm^{-1}): 3367, 3027, 2214, 1595, 1539, 1492, 1413, 1222, 989, 938, 889, 821, 739, 687. GC–MS (EI) m/z: 280 $[M]^+$. Elemental anal. calcd for $C_{20}H_{12}N_2\,0.2H_2O$: C, 84.60; H, 4.40; N, 9.87. Found: C, 84.79; H, 4.42; N, 9.61.

Self-assembly of Complex 2a

Compound **1a** (6.34 mg, 14.2 μmol) was treated with $Pd(NO_3)_2$ (1.64 mg, 7.12 μmol) in DMSO (0.7 ml) at 70°C for 2 h. The quantitative formation of complex **2a** was confirmed by ^{1}H NMR. The title compound was precipitated as an ochre solid by adding diethyl ether to the solution, filtrated and dried *in vacuo*. Isolated yield was 6.90 mg (0.514 μmol, 87%): m.p. > 190°C (decomposed). ^{1}H NMR (500 Hz, DMSO-d_6) δ: 9.28 (br s, 96H), 7.88 (br s, 96H), 7.74 (br s, 48H), 7.34 (br s, 24H), 4.75 (br s, 48H), 3.97 (br s, 48H), 3.30 (br s, 216H). ^{13}C NMR (125 MHz, DMSO-d_6) δ: 159.6 (C), 151.3 (CH), 137.0 (CH), 134.0 (C), 128.7 (CH), 125.1 (CH), 114.3 (C), 93.5 (C), 90.3 (C), 67.8 (CH_2), 64.6 (CH_2), 53.2 (CH_3). Diffusion coefficient: $D = 4.7 \times 10^{-11}$ $m^2\,s^{-1}$. IR (KBr, cm^{-1}): 3033, 2357, 2214, 1726, 1610, 1493, 1385, 1228, 1204, 1063, 1042, 954, 903, 875, 826, 793, 749, 553, 512. Mass spectrometry was performed after complex **2a** was converted to its $CF_3SO_3^-$ salt by adding saturated aqueous CF_3SO_3Na to the DMSO solution of complex **2a**. CSI-MS ($CF_3SO_3^-$ salt, CH_3CN): m/z 2367.8 $[M - 7(CF_3SO_3^-)]^{7+}$, 2053.1 $[M - 8(CF_3SO_3^-)]^{8+}$, 1808.4 $[M - 9(CF_3SO_3^-)]^{9+}$, 1612.7 $[M - 10(CF_3SO_3^-)]^{10+}$, 1452.5 $[M - 11(CF_3SO_3^-)]^{11+}$. Elemental anal. calcd for $C_{600}H_{576}N_{120}O_{168}Pd_{12}$ 35-DMSO: C, 49.77; H, 4.90; N, 10.35. Found: C, 49.89; H, 4.90; N, 10.21.

Self-assembly of Complex 2b

A similar procedure to that of complex **2a** was employed to compound **1b** (2.28 mg, 6.00 μmol) to give complex **2b**. Isolated yield was 2.30 mg (0.462 μmol, 77%): m.p. > 200°C (decomposed). ^{1}H NMR (500 MHz, DMSO-d_6) δ: 9.24 (br s, 96H), 7.78 (br s, 96H), 7.70 (br s, 48H), 7.28 (br s, 24H), 4.28 (br s, 48H), 1.83 (br s, 48H), 0.94 (br s, 216H). ^{13}C NMR (125 MHz, DMSO-d_6) δ: 162.2 (C), 151.2 (CH), 136.3 (CH), 134.1 (C), 128.3 (CH), 124.6 (CH), 115.2 (C), 94.0 (C), 89.6 (C), 72.6 (CH_2), 42.8 (CH_2), 29.5 (CH_3), 29.4 (C). Diffusion coefficient: $D = 4.0 \times 10^{-11}$ $m^2\,s^{-1}$. IR (KBr, cm^{-1}): 2960, 2933, 2861, 2213, 1727, 1611, 1500, 1464, 1442, 1384, 1274, 1204, 1124, 1073, 1040, 961, 834, 791, 745, 706. Mass spectrometry was performed after the same treatment to that of **2a**. CSI-MS ($CF_3SO_3^-$ salt, CH_3CN): m/z 3347.2 $[M - 4(CF_3SO_3^-)]^{4+}$, 2647.9 $[M - 5(CF_3SO_3^-)]^{5+}$, 2181.6 $[M - 6(CF_3SO_3^-)]^{6+}$, 1848.7 $[M - 7(CF_3SO_3^-)]^{7+}$, 1598.9 $[M - 8(CF_3SO_3^-)]^{8+}$, 1404.7 $[M - 9(CF_3SO_3^-)]^{9+}$, 1249.3 $[M - 10(CF_3SO_3^-)]^{10+}$, 1122.1 $[M - 11(CF_3SO_3^-)]^{11+}$,

1016.2 $[M - 12(CF_3SO_3^-)]^{12+}$. Elemental anal. calcd for $C_{624}H_{576}N_{72}O_{96}Pd_{12}$ 18DMSO: C, 60.23; H, 5.10; N, 7.46. Found: C, 60.47; H, 5.08; N, 7.27.

Self-assembly of Complex 2c

A similar procedure to that of complex **2a** was employed to compound **1c** (5.60 mg, 20.0 μmol) to give complex **2c**. Isolated yield was 7.11 mg (0.750 μmol, 90%): m.p. > 200°C (decomposed). ^{1}H NMR (500 MHz, DMSO-d_6) δ: 9.23 (br s, 96H), 7.90 (br s, 24H), 7.86 (br s, 96H), 7.72 (br s, 48H), 7.49 (br s, 24H). ^{13}C NMR (125 MHz, DMSO-d_6) δ: 151.1 (CH), 135.7 (CH), 134.0 (C), 133.8 (CH), 130.0 (CH), 128.7 (CH), 121.1 (C), 96.6 (C), 86.1 (C). Diffusion coefficient: $D = 4.0 \times 10^{-11}$ m^2 s^{-1}. IR (KBr, cm^{-1}): 3096, 3050, 2924, 2853, 2214, 1611, 1500, 1384, 1340, 1274, 1214, 1168, 1124, 1063, 1041, 989, 836, 800, 683. Mass spectrometry was performed after the same treatment to that of **2a**. CSI-MS ($CF_3SO_3^-$ salt, CH_3CN): m/z 2167.3 $[M - 5(CF_3SO_3^-)]^{5+}$, 1781.2 $[M - 6(CF_3SO_3^-)]^{6+}$, 1505.5 $[M - 7(CF_3SO_3^-)]^{7+}$, 1298.7 $[M - 8(CF_3SO_3^-)]^{8+}$, 1137.8 $[M - 9(CF_3SO_3^-)]^{9+}$, 1009.2 $[M - 10(CF_3SO_3^-)]^{10+}$, 903.9 $[M - 11(CF_3SO_3^-)]^{11+}$, 816.1 $[M - 12(CF_3SO_3^-)]^{12+}$, 741.8 $[M - 13(CF_3SO_3^-)]^{13+}$. Elemental anal. calcd for $C_{480}H_{288}N_{72}O_{72}Pd_{12}$ 42DMSO: C, 54.81; H, 4.10; N, 7.24. Found: C, 54.51; H, 3.72; N, 7.24.

Typical Procedure for Radical Polymerisation in Spherical Complexes

A DMSO solution (6.0 ml) containing complex **2a** or **2b** (2.50 μmol, 0.417 mM), sodium *p*-styrenesulphonate **8** (123 mg, 0.597 mmol, 99.4 mM) and $NaHSO_3$ (0.68 mg, 6.5 μmol, 1.1 mM) in a Schlenk tube was subjected to repeated freeze–thaw cycles, and then a DMSO solution (60 μl) of $(NH_4)_2S_2O_8$ (6.0 μmol) was added into the mixed solution before polymerisation. Polymerisation was quenched rapidly by immersing the Schlenk tube into liquid nitrogen bath after 2 h heating at 70°C.

Decomposition of Cation/anion Complexes and Purification of Anionic Polymers

Complex **2a** or **2b**/PSS complexes in polymerisation solution (0.6 ml) were thoroughly precipitated by adding acetone and dried under reduced pressure. The polyelectrolyte complex were decomposed by adding ethylenediamine (5 μl) and the resultant mixture was extracted with water (0.6 ml). Insoluble mixtures were filtered off and the crude solution was purified by cation exchange chromatography (H-form) to give poly(styrenesulphonic acid). The acidic polymer was neutralised with aqueous NaOH and the resultant sample solution was lyophilised to afford a purified PSS powder.

Supplementary Materials

NMR spectra of the complex **2a**, DOSY spectra on the encapsulation experiments and NMR spectra on the polymerisation experiments are available as supplementary materials.

Acknowledgements

This research is supported by the CREST project of the Japan Science and Technology Agency (JST) and by the Ministry of Education, Culture, Sports, Science and Technology of Japan.

References

[1] Speir, J. A.; Munshi, S.; Wang, G.; Baker, T. S.; Johnson, J. E. *Structure* **1995**, *3*, 63.
[2] Konecny, R.; Trylska, J.; Tama, F.; Zhang, D.; Baker, N. A.; Brooks, III, C. L.; McCammon, J. A. *Biopolymers* **2006**, *82*, 106.
[3] Holmberg, K.; Jönsson, B.; Kronberg, B.; Lindman, B. *Surfactants and Polymers in Aqueous Solution*;, 2nd ed. John Wiley & Sons: England, 2003; pp 1–37.
[4] Beck, J. S.; Vartuli, J. C.; Roth, W. J.; Leonowicz, M. E.; Kresge, C. T.; Schmitt, K. D.; Chu, C. T. -W.; Olson, D. H.; Sheppard, E. W.; McCullen, S. B.;, et al., *J. Am. Chem. Soc.* **1992**, *114*, 10834.
[5] Kresge, C. T.; Leonowicz, M. E.; Roth, J.; Vartuli, J. C.; Beck, J. S. *Nature* **1992**, *359*, 710.
[6] Soler-Illia, G. J.; de, A. A.; Sanchez, C.; Lebeau, B.; Patarin, J. *Chem. Rev.* **2002**, *102*, 4093.
[7] van Bommel, K. J. C.; Friggeri, A.; Shinkai, S. *Angew. Chem. Int. Ed.* **2003**, *42*, 980.
[8] Higashi, N.; Adachi, T.; Niwa, M. *Macromolecules* **1988**, *21*, 2297.
[9] Higashi, N.; Adachi, T.; Niwa, M. *Macromolecules* **1990**, *23*, 1475.
[10] Tajima, K.; Aida, T. *Chem. Commun.* **2006**, 2399.
[11] Kline, S. R. *Langmuir* **1999**, *15*, 2726.
[12] Gerber, M. J.; Kline, S. R.; Walker, L. M. *Langmuir* **2004**, *20*, 8510.
[13] Gerber, M. J.; Walker, L. M. *Langmuir* **2006**, *22*, 941.
[14] Kim, T.-H.; Choi, S. -M.; Kline, S. R. *Langmuir* **2006**, *22*, 2844.
[15] Blumstein, A.; Kakivaya, S. R.; Shah, K. R. *J. Polym. Sci. Symp.* **1974**, *45*, 75.
[16] Blumstein, A.; Kakivaya, S. R.; Salamone, J. C. *J. Polym. Sci., Polym. Lett. Ed.* **1974**, *12*, 651.
[17] Blumstein, A.; Weill, G. *Macromolecules* **1977**, *10*, 75.
[18] Blumstein, A.; Ponrathnam, S.; Bellantoni, E. *J. Polym. Sci., Polym. Lett. Ed.* **1980**, *18*, 299.
[19] Douglas, T.; Young, M. *Nature* **1998**, *393*, 152.
[20] Douglas, T.; Young, M. *Adv. Mater.* **1999**, *11*, 679.
[21] Douglas, T.; Young, M. *Adv. Mater.* **2002**, *14*, 415.
[22] Allen, M.; Willits, D.; Mosolf, J.; Young, M.; Douglas, T. *Adv. Mater.* **2002**, *14*, 1562.
[23] Douglas, T.; Young, M. *Science* **2006**, *312*, 873.
[24] Kim, J. -W.; Choi, S. H.; Lillehei, P. T.; Chu, S. -H.; King, G. C.; Watt, G. D. *Chem. Commun.* **2005**, 4101.
[25] Uchida, M.; Klem, M. T.; Allen, M.; Suci, P.; Flenniken, M.; Gillitzer, E.; Varpness, Z.; Liepold, L. O.; Young, M.; Douglas, T. *Adv. Mater.* **2007**, *19*, 1025.
[26] Flenniken, M. L.; Liepold, L. O.; Crowley, B. E.; Willits, D. A.; Young, M. J.; Douglas, T. *Chem. Commun.* **2005**, 447.
[27] Hooker, J. M.; Kovacs, E. W.; Francis, M. B. *J. Am. Chem. Soc.* **2004**, *126*, 3718.
[28] Gillitzer, E.; Willits, D.; Young, M.; Douglas, T. *Chem. Commun.* **2002**, 2390.
[29] Chatterji, A.; Ochoa, W. F.; Paine, M.; Ratna, B. R.; Johnson, J. E.; Lin, T. *Chem. Biol.* **2004**, *11*, 855.
[30] Wang, Q.; Raja, K. S.; Janda, K. D.; Lin, T.; Finn, M. G. *Bioconjugate Chem.* **2003**, *14*, 38.

[31] Zeng, Q.; Li, T.; Cash, B.; Li, S.; Xie, F.; Wang, Q. *Chem. Commun.* **2007**, 1453.
[32] Tominaga, M.; Suzuki, K.; Kawano, M.; Kusukawa, T.; Ozeki, T.; Sakamoto, S.; Yamaguchi, K.; Fujita, M. *Angew. Chem. Int. Ed.* **2004**, *43*, 5621.
[33] Tominaga, M.; Suzuki, K.; Murase, T.; Fujita, M. J. *Am. Chem. Soc.* **2005**, *127*, 11950.
[34] Sato, S.; Iida, J.; Suzuki, K.; Kawano, M.; Ozeki, T.; Fujita, M. *Science* **2006**, *313*, 1273.
[35] Murase, T.; Sato, S.; Fujita, M. *Angew. Chem. Int. Ed.* **2007**, *46*, 1083.
[36] Kamiya, N.; Tominaga, M.; Sato, S.; Fujita, M. *J. Am. Chem. Soc.* **2007**, *129*, 3816.
[37] Murase, T.; Sato, S.; Fujita, M. *Angew. Chem. Int. Ed.* **2007**, *46*, 5133.
[38] Gray, A. P.; Platz, R. D.; Chang, T. C. P.; Leverone, T. R.; Ferrick, D. A.; Kramerll, D. N. *J. Med. Chem.* **1985**, *28*, 111.
[39] Wu, D.; Chen, A.; Johnson, Jr, C. S. *J. Magn. Reson., Ser. A* **1995**, *115*, 260.
[40] Sakamoto, S.; Fujita, M.; Kim, K.; Yamaguchi, K. *Tetrahedron* **2000**, *56*, 955.
[41] Saito, R.; Yamaguchi, K. *Macromolecules* **2003**, *36*, 9005.
[42] Wiley, R. H.; Smith, N. R.; Ketterer, C. C. *J. Am. Chem. Soc.* **1954**, *76*, 720.
[43] Izumi, Z.; Kiuchi, H.; Watanabe, M. *J. Polym. Sci., Part* **1963**, *1*, 705.
[44] Izumi, Z.; Kiuchi, H.; Watanabe, M.; Uchiyama, H. *J. Polym. Sci., Part A: Gen. Pap* **1965**, *3*, 2721.
[45] Kurenkov, V. F.; Orlova, G. P.; Myagchenkov, V. A. *Eur. Polym. J.* **1978**, *14*, 657.
[46] Danis, P. O.; Karr, D. E. *Macromolecules* **1995**, *28*, 8548.
[47] Yang, J. C.; Mays, J. W. *Macromolecules* **2002**, *35*, 3433.
[48] Cong, R.; Turksen, S.; Russo, P. *Macromolecules* **2004**, *37*, 4731.
[49] Sarac, A. S. *Prog. Polym. Sci.* **1999**, *24*, 1149.